Switching brain serotonin with oxytocin

Raphaelle Mottolese[a,b], Jérôme Redouté[b,c], Nicolas Costes[c], Didier Le Bars[b,c], and Angela Sirigu[a,b,1]

[a]Center for Cognitive Neuroscience, Unité Mixte de Recherche 5229, Centre National de la Recherche Scientifique, 69675 Bron, France; [b]University Claude Bernard Lyon 1, 69609 Lyon, France; and [c]Centre d'Etude et de Recherche Multimodal et Pluridisciplinaire Imagerie du Vivant, 69003 Lyon, France

Edited by Leslie G. Ungerleider, National Institute of Mental Health, Bethesda, MD, and approved April 29, 2014 (received for review October 22, 2013)

Serotonin (5-HT) and oxytocin (OXT) are two neuromodulators involved in human affect and sociality and in disorders like depression and autism. We asked whether these chemical messengers interact in the regulation of emotion-based behavior by administering OXT or placebo to 24 healthy subjects and mapping cerebral 5-HT system by using 2′-methoxyphenyl-(N-2′-pyridinyl)-p-[^{18}F]fluoro-benzamidoethylpiperazine ([^{18}F]MPPF), an antagonist of 5-HT$_{1A}$ receptors. OXT increased [^{18}F]MPPF nondisplaceable binding potential (BP$_{ND}$) in the dorsal raphe nucleus (DRN), the core area of 5-HT synthesis, and in the amygdala/hippocampal complex, insula, and orbitofrontal cortex. Importantly, the amygdala appears central in the regulation of 5-HT by OXT: [^{18}F]MPPF BP$_{ND}$ changes in the DRN correlated with changes in right amygdala, which were in turn correlated with changes in hippocampus, insula, subgenual, and orbitofrontal cortex, a circuit implicated in the control of stress, mood, and social behaviors. OXT administration is known to inhibit amygdala activity and results in a decrease of anxiety, whereas high amygdala activity and 5-HT dysregulation have been associated with increased anxiety. The present study reveals a previously unidentified form of interaction between these two systems in the human brain, i.e., the role of OXT in the inhibitory regulation of 5-HT signaling, which could lead to novel therapeutic strategies for mental disorders.

Brain chemistry strongly influences our behavior. Among neuromodulators, serotonin (5-HT) and oxytocin (OXT) are important for the regulation and expression of several behaviors such as human affects and socialization. Both systems have been implicated in the control of stress, anxiety, and social cooperation (1, 2). Moreover, their dysfunction is associated with major psychiatric disorders such as depression (3, 4) and autism (5, 6). Recent animal studies demonstrated that specific anatomical links exist between these two molecules. Serotonergic fibers originating from the dorsal and medial raphe nuclei of the brainstem project toward magnocellular neurons in the paraventricular and supraoptic nuclei of the hypothalamus, where OXT is released (7). In this region, 5-HT fibers overlap and follow the distribution of OXT cells (8). Importantly, in the raphe nuclei, the core area of 5-HT synthesis, serotonergic neurons display OXT receptors and OXT modulates the release of 5-HT (9). Recent results have also shown that administration of OXT during the postnatal period increases the length of serotonergic axons in the hypothalamus and in the amygdala (10). In return, 5-HT is able to modulate OXT release while interacting with different 5-HT receptors in the hypothalamus (11). Also, the administration of fenfluramine, a serotonergic agonist, to healthy subjects increases plasma OXT level (12). These findings indicate that OXT and 5-HT share anatomical substrates, which may constitute a functional interface in the regulation of emotion-based behaviors. Behaviorally, OXT and 5-HT modulate reactions to social contexts and threatening stimuli in humans and animals (13, 14). For instance, oversensitivity to threat-related contexts, a mark of mood and anxiety disorders, is mediated by 5-HT in the amygdala, a region important for fear and fear conditioning response (15). OXT suppresses amygdala response to emotionally threatening stimuli such as faces or scenes (16), and has anxiolytic effects (14). 5-HT and OXT systems are involved in the avoidance/approach motivational system: 5-HT has been implicated in the regulation of defensive, aversive, and harm avoidance behavior (13), and OXT is known for its role in affiliative behavior and proximity maintenance (1). Although no data are available in humans, this raises the question whether 5-HT and OXT work strictly independently on approach and avoidance systems or whether they show mutual interactions for regulating the balance between these opposite behavioral tendencies.

In a randomized double-blind investigation, we administered placebo or intranasal OXT to 24 healthy male subjects. We have chosen to enroll male subjects only to avoid the confounding effects linked to sex and a possible interaction with gonadal steroids. Indeed, as shown by previous studies, OXT modulates brain activity differently in male and female subjects. For instance, OXT suppresses amygdala response to emotionally threatening stimuli in males but enhances the same response in females (16, 17). We mapped the 5-HT$_{1A}$ system by using PET with 2′-methoxyphenyl-(N-2′-pyridinyl)-p-[^{18}F]fluoro-benzamidoethylpiperazine ([^{18}F]MPPF), a selective antagonist of 5-HT$_{1A}$ auto- and heteroreceptors. With this method, we measured, through PET imaging, OXT-induced variation on [^{18}F]MPPF nondisplaceable binding potential (BP; BP$_{ND}$) in regions known to be rich in 5-HT$_{1A}$. In line with current occupancy models, increased MPPF BP$_{ND}$ means more availability for the antagonist to bind at the receptor level and accordingly diminished 5-HT central concentration (18). The 5-HT$_{1A}$ system located in raphe nuclei and in projection areas, amygdala, hippocampus, parahippocampus, insula, and cingular and prefrontal cortex (18, 19) contains neurons that carry inhibitory signals to regulate synaptic release of 5-HT (20). This system is of particular interest here because reduced expression of 5-HT$_{1A}$ receptors has been linked to an "anxious" phenotype (21). Also, 5-HT$_{1A}$ receptor binding is decreased in patients with depression (3) or social anxiety (22), two disorders in which OXT is considered as having a potential therapeutic benefit (1, 4). We therefore expected the 5-HT$_{1A}$ system to be a significant target for OXT action.

Results

OXT Effect on 5-HT$_{1A}$ Receptor Brain Mapping. All subjects underwent a first scan to evaluate the basal distribution of 5-HT$_{1A}$ receptors (basal-state condition). A second scan was performed

Significance

Serotonin (5-HT) and oxytocin (OXT) are two neuromodulators involved in human affect and sociality and in disorders like depression and autism. Here we show that these chemical messengers interact in areas of the human brain important for the regulation of emotion-based behavior. By highlighting the role of OXT in the regulation of 5-HT signaling, our findings can lead to novel therapeutic strategies for mental disorders such as social anxiety, depression, and autism.

Author contributions: R.M. and A.S. designed research; R.M., J.R., D.L.B., and A.S. performed research; R.M., J.R., N.C., and A.S. analyzed data; and R.M., J.R., N.C., and A.S. wrote the paper.

The authors declare no conflict of interest.

This article is a PNAS Direct Submission.

[1]To whom correspondence should be addressed. E-mail: sirigu@isc.cnrs.fr.

1 wk later with subjects receiving 24 IU of intranasal OXT (OXT group, $n = 12$) or placebo (placebo group, $n = 12$). Fig. 1, *Upper*, shows the mean BP_{ND} obtained during the basal state for all subjects. We used MarsBar toolbox (23) to extract regional mean MPPF BP_{ND} from regions shown in a healthy population database (24) to be key nodes of the 5-HT_{1A} system and from the basal-state results obtained in our subjects (Fig. 1, *Upper*). These include dorsal raphe nucleus (DRN), left and right amygdala/hippocampus/parahippocampus complex, insula, anterior/medial cingulate, and orbitofrontal cortex. The boundaries of these regions of interest (ROIs) were identified by using the Hammersmith N30R83 maximum probability atlas (25). The DRN was anatomically outlined from the functional image found in the basal state (*Materials and Methods* and Fig. 1, *Upper*) because the Hammersmith atlas does not cover this region. No differences were found in the basal MPPF BP_{ND} between the two groups (OXT/placebo; $P > 0.05$, two-sample t test). In a combined contrast [(OXT after spray − basal OXT) − (placebo after spray − basal placebo)], we found that OXT administration induced a significant mean MPPF BP_{ND} increase of 3.22% ± 9.64, which was statistically higher ($P < 0.0001$) than the nonsignificant mean variation observed in the placebo group (0.04% ± 9.10). MPPF BP_{ND} variations after spray (OXT or placebo) compared with the basal state were assessed with one-sample t tests. This test was performed on the relative MPPF BP_{ND} variation within the ROIs, with the null hypothesis that there were no differences between the basal and spray conditions. No significant MPPF BP_{ND} variation was observed in the placebo group compared with the basal state (all $P > 0.05$; Table 1). In contrast, in the group receiving OXT, MPPF BP_{ND} significantly increased in the DRN (+6.51% ± 11.91; $P < 0.05$), the core area of 5-HT synthesis; in the right amygdala/hippocampus/parahippocampus complex (+3.03% ± 4.27; $P < 0.05$); in the right (+3.71% ± 5.64; $P < 0.05$) and left (+1.92% ± 3.54; $P < 0.05$) insula; and in the right medioventral orbitofrontal cortex (+3.61% ± 6.37; $P < 0.05$; Table 1). Fig. 1, *Lower*, obtained with SPM analysis, is provided to illustrate the localization of MPPF BP_{ND} variation after OXT at the voxel level.

Between-Region Correlation After OXT. To examine whether the magnitude of OXT effect in DRN correlated with the MPPF BP_{ND} in these latter regions, we entered the individual mean MPPF BP_{ND} values as a covariate (voxel-based analysis) by using a linear regression model (26). Under OXT, we found a significant correlation between MPPF BP_{ND} in the DRN, our seed region (Fig. 2, *Left*), and that in right amygdala (voxel threshold, $P < 0.01$; cluster threshold, $k \geq 127$; cluster size, $k_E = 773$; peak voxel, $x, y, z = 24, 2, -20$; $P < 0.002$), suggesting a functional linkage between effects of OXT on 5-HT in the two regions (Fig. 2, *Right*). No significant correlation was found in the basal state or in the placebo group.

In turn, correlation analysis with right amygdala MPPF BP_{ND} as seed region showed covariations in the right hippocampus, right insula, and right medioventral orbitofrontal cortex (Table 2). Another region, the subgenual cortex, whose main response to OXT was near significance (right subgenual, $P < 0.07$; left subgenual, $P < 0.09$) also correlated bilaterally with right amygdala (Table 2). No correlation was found in the placebo group or in the OXT group at basal state for any of these comparisons.

Discussion

These findings show that OXT modulates the serotoninergic system. If the interaction between these neuromodulators has been shown in the past by animal research, to our knowledge, this is the first study to reveal similar effects in the human brain. The finding that OXT regulates 5-HT_{1A} network suggests that OXT interferes with 5-HT neurotransmission. In accordance with occupancy models, an increase of MPPF BP_{ND} means that more space is available for the antagonist to bind at the 5-HT_{1A} receptor, and this in turn reflects depletion of 5-HT in the extracellular space (18). We show that OXT exerts an action at the very root of the 5-HT system, as demonstrated by the increase of MPPF BP_{ND} in the DRN, the main locus of 5-HT synthesis (20). In line with this, increased 5-HT concentration induced by the 5-HT reuptake inhibitor fluoxetine reduces MPPF BP_{ND} in the DRN (27). Consequently, the increase of MPPF BP_{ND} observed here could be interpreted as an inhibitory effect of OXT on 5-HT activity. Along the same line, rats treated

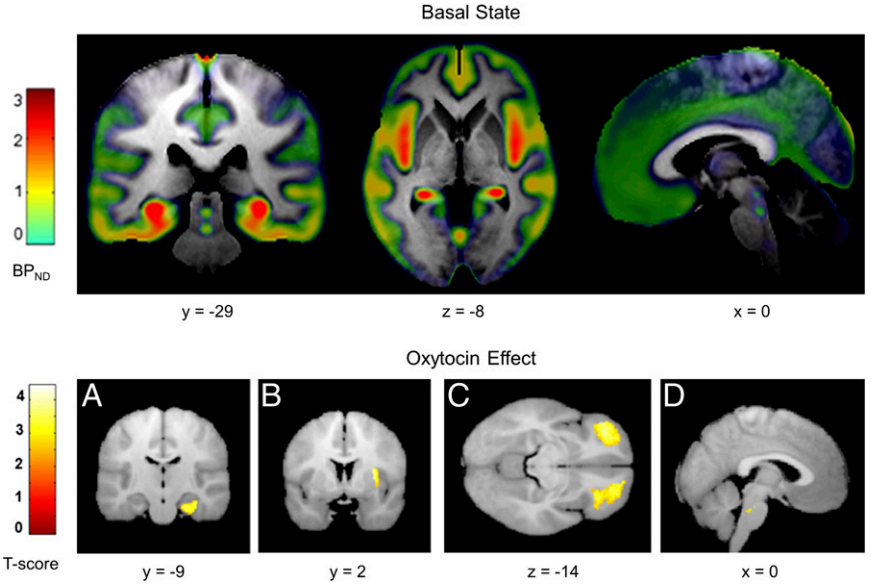

Fig. 1. MPPF binding on 5-HT_{1A} receptors in the basal state and OXT effect. (*Upper*) Brain mapping of the MPPF binding potential (BP_{ND}) in the basal state ($n = 24$). 5-HT_{1A} binding is localized in amygdala, hippocampus and parahippocampus, insula, DRN, orbitofrontal cortex, and anterior cingulate cortex. (*Lower*) T-map SPM analysis ($P < 0.01$) showing the effect of OXT administration on MPPF BP_{ND} in the OXT group (n = 12) compared with the basal state: (*A*) right amygdala/hippocampus/parahippocampus complex, (*B*) right anterior insula, (*C*), right and left orbitofrontal cortex, and (*D*) DRN. No significant effect in the placebo group ($n = 12$) was found. For regional statistical results, see Table 1. PET images are mapped on the averaged individual MRI scans.

Table 1. MPPF regional BP_{ND} at basal state and after spray and relative variations after spray

Region/side/group	MPPF BPND		Relative variation, %	*P* value
	Basal state	After spray		
Amygdala–hippocampus–parahippocampus complex				
Right				
OXT	1.58 ± 0.11	1.63 ± 0.13	3.03 ± 4.27	0.016*
Placebo	1.56 ± 0.16	1.55 ± 0.15	−0.36 ± 4.82	0.601
Left				
OXT	1.55 ± 0.10	1.57 ± 0.11	1.02 ± 4.52	0.226
Placebo	1.53 ± 0.14	1.52 ± 0.15	−0.45 ± 4.94	0.621
Insula				
Right				
OXT	0.83 ± 0.06	0.86 ± 0.06	3.71 ± 5.64	0.022*
Placebo	0.83 ± 0.10	0.84 ± 0.10	1.10 ± 8.61	0.334
Left				
OXT	0.76 ± 0.06	0.78 ± 0.07	1.92 ± 3.54	0.044*
Placebo	0.78 ± 0.09	0.78 ± 0.10	0.81 ± 7.19	0.351
DRN				
OXT	0.43 ± 0.11	0.46 ± 0.12	6.51 ± 11.91	0.042*
Placebo	0.40 ± 0.08	0.40 ± 0.09	0.98 ± 13.86	0.405
Orbitofrontal cortex (mid-/ventral)				
Right				
OXT	0.78 ± 0.10	0.81 ± 0.10	3.63 ± 6.55	0.041*
Placebo	0.77 ± 0.10	0.76 ± 0.10	−1.11 ± 8.19	0.676
Left				
OXT	0.76 ± 0.09	0.79 ± 0.11	3.28 ± 6.44	0.053
Placebo	0.77 ± 0.11	0.76 ± 0.11	−0.78 ± 7.47	0.638
Anterior cingulate cortex (midpregenual–subgenual)				
Right				
OXT	0.72 ± 0.07	0.73 ± 0.07	2.21 ± 4.89	0.073
Placebo	0.71 ± 0.10	0.71 ± 0.09	0.02 ± 6.74	0.497
Left				
OXT	0.71 ± 0.08	0.73 ± 0.06	2.97 ± 7.29	0.093
Placebo	0.70 ± 0.10	0.70 ± 0.10	0.52 ± 7.51	0.408

P values of regional variation were determined with a one-sample *t* test on the relative variation.
*$P < 0.05$.

with a 5-HT agonist (5-methoxytryptamine), which causes hyperserotonemia, exhibit a decrease of OXT in the paraventricular nucleus of the hypothalamus and a form of "autistic-like" behavior (28), suggesting the existence of mutual interactions between the 5-HT and OXT systems.

Different mechanisms may be involved in the observed most likely inhibitory effects of OXT on 5-HT. One possible route is by direct interference with 5-HT neuronal activity in the raphe nuclei, leading to a reduction of 5-HT secretion in the extracellular space. However, a decrease of 5-HT concentration in raphe nuclei would result in lower stimulation of 5-HT_{1A} autoreceptors and a consequent relative increase of 5-HT concentration in projections areas (18, 29), which is not the case in the present study. Alternatively, an increase of 5-HT_{1A} autoreceptor availability and/or affinity in raphe nuclei could explain and reinforce the increase of the MPPF BP_{ND} in projection areas after OXT, leading to a 5-HT decrease in these regions. At a methodological level, there are now a fair number of animal and human studies in favor of the sensitivity of MPPF binding to endogenous 5-HT variations. For instance, Zimmer et al. showed in rodents that [^{18}F]MPPF kinetic decreases after experimental depletion of endogenous 5-HT (30). Another study found, in healthy men, a significant correlation between MPPF BP in 5-HT_{1A} and 5-HT synthesis bilaterally in hippocampus, anterior insula, and left anterior cingulate cortex (31), suggesting that an increase of 5-HT correlates with a decrease of the MPPF BP. It should be stressed that contradictory evidence has been also reported on an earlier study by Udo De Haes et al., who failed to find significant changes in MPPF BP after 5-HT level manipulation using tryptophan depletion (32). However, as acknowledged by the authors, the large interindividual variability they found in their study and the limited impact of their tryptophan manipulation on 5-HT expression limit the general validity of their conclusions. Thus, our results are rather in favor of the hypothesis that an increase of MPPF BP_{ND} is a direct consequence of OXT action on 5-HT_{1A} receptors by increasing, for instance, their availability and/or affinity.

Given that 5-HT neurons in the raphe nuclei display OXT receptors (9), an interaction between the two neuromodulators at the receptors level is likely. 5-HT_{1A} receptors can exist in a high-affinity state (G protein-coupled 5-HT_{1A} receptors) and a low-affinity state (free 5-HT_{1A} receptors) (33). We can speculate that OXT action activates, through its receptors, a cell signaling pathway that leads to the coupling of 5-HT_{1A} free receptors to a G protein. In order words, OXT might help the transition between the low- and high-affinity states of 5-HT_{1A} receptors, thus enhancing their signaling force. Although this remains a speculative hypothesis, it certainly deserves further investigation.

Within 5-HT_{1A} projection areas, the right amygdala may play a strategic role in OXT modulation of the 5-HT pathway. Administration of OXT inhibits the right amygdala activity during perception of stressful scenes (16), whereas high amygdala activity has been associated with increased anxiety (15), which is also a hallmark of 5-HT dysregulation (34). In agreement with this point, induced psychological stress in mice has been found to increase extracellular 5-HT levels in amygdala (35). Thus, right amygdala seems to be a key site for the interaction between OXT and 5-HT, and we can speculate that the well-known anxiolytic effect of OXT (14) is mediated by its modulation of the 5-HT activity in the amygdala.

Importantly, we also found that OXT-induced changes in 5-HT_{1A} signaling in the right amygdala are correlated with changes in the DRN on the one hand, and in several limbic and cortical areas on the other hand. Functionally, amygdala and DRN seem to entertain a privileged relation. Compared with the basal state and with placebo, OXT significantly increased the functional coupling between the two regions. There are known dense projections from raphe nuclei to the amygdala (36). Recently, it has been shown that an increase of 5-HT_{1A} BP_{ND} with [^{11}C]WAY100635 (another 5-HT_{1A} antagonist with higher affinity) in the DRN predicts a decrease in amygdala bold signal reactivity (29). Our results are in keeping with this finding, and go further by demonstrating that OXT is a major player in the functional link between DRN and amygdala, suggesting that amygdala reactivity may be crucial in the cascade of effects triggered by OXT on the 5-HT_{1A} system.

We also found that variations of MPPF BP_{ND} in the right amygdala are correlated with MPPF BP_{ND} variation in right hippocampus, right insula, and right orbitofrontal cortex, a circuit important for regulating emotion, bodily stress, and impulse inhibition (37). The relevance of this functional circuit for OXT's action has been shown in a previous functional MRI study that indicated that connectivity between these regions and the amygdala is increased under OXT (38). Our results go beyond this and suggest that OXT increases such functional connectivity through its regulation of the 5-HT_{1A} pathway.

In addition, amygdala and hippocampus form a unique anatomical complex, and both are important targets of OXT and 5-HT (18). The hippocampus displays a high level of 5-HT_{1A} receptors (21, 34). Inactivation of the 5-HT_{1A} autoreceptors in transgenic mice is associated with increased anxiety and stress activity (34). However, when restoring 5-HT_{1A} expression and

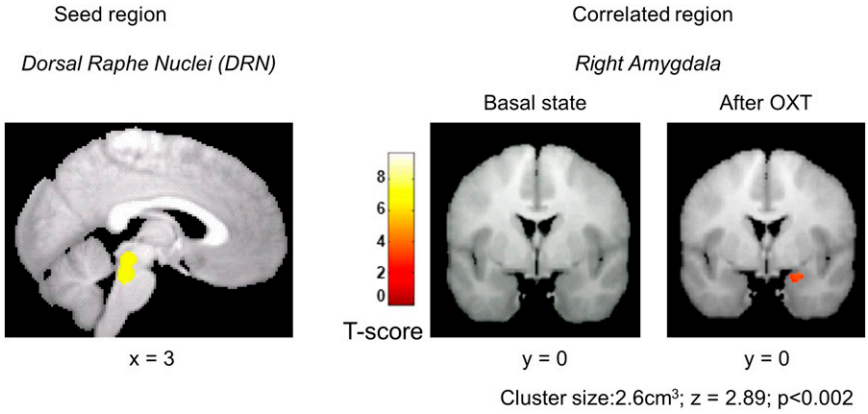

Fig. 2. MPPF BP_{ND} correlation of DRN with right amygdala. (*Left*) Seed region: DRN was identified by selecting on the average PET BP_{ND} image at the basal state, the connected voxels exceeding 80% of the maximum value in the brainstem. The individual MPPF BP_{ND} values in DRN were used to find voxels covarying within our ROIs. (*Right*) Correlated region: after OXT, we observed a cluster of voxels (1 voxel = 3.375 mm^3) with a significant positive correlation in the right amygdala (voxel threshold, $P < 0.01$; cluster size, $k \geq 127$ voxels). No correlation was found in the basal state in the OXT group. No significant correlation was found in the placebo group at basal state or after placebo spray.

activity in the hippocampus, the normal phenotype of the KO mice is rescued (21). Notably, OXT injection in this area suppresses freezing behavior (39), a reaction to fear and stressful conditions. Our results suggest that amygdala and hippocampus constitute a common ground where OXT and 5-HT interactions could regulate the response to stress and anxiety.

In the present study, OXT also enhanced the functional coupling of 5-HT activity in the right amygdala and cortical regions such as the insula and the medioventral orbitofrontal cortex, which are involved in a range of behaviors, including pain, social emotions processing, impulsivity, and inhibitory control (37). In particular, we found effects of OXT on the right orbitofrontal cortex, which receives strong projections from the amygdala (40) as well as from the DRN (41). In patients with anxiety disorder, Hahn et al. found an altered regulation of the orbitofrontal cortex through 5-HT_{1A} raphe autoreceptors (42). Although our results do not show a functional correlation between the orbitofrontal cortex and the DRN, but rather between amygdala and orbitofrontal cortex, they emphasize the importance of this region in OXT and 5-HT regulation. Finally, the left and right subgenual cortices, whose main response to OXT was near significance, also correlated with right amygdala, and, again, such a correlation was not found in the placebo group or in the OXT group during the basal state. We know that amygdala and the subgenual frontal cortex are anatomically connected (43). Like the amygdala, the subgenual region is known to be implicated in mood disorders such as anxiety (44), and deep stimulation of this region alleviates depression (45), a psychiatric condition in which OXT has beneficial effects on anxiety symptoms (46). Our results show that OXT administration functionally links these two regions and suggest that OXT effects on 5-HT_{1A} within the subgenual cortex could be mediated by induced OXT effects occurring in the amygdala. This hypothesis remains highly speculative, but it is worthy to pursue given the key role of these areas in emotional disturbances.

In view of these findings, we propose that OXT is linked to 5-HT by a reciprocal and coordinated functional relation similar to the links previously evoked between OXT and cortisol (47) or OXT and estrogen (48). This may be of relevance to psychiatric research. Indeed, the therapeutic potential of OXT has been demonstrated in autism (49), social anxiety disorders, impulse aggressivity, and depression (1, 4). Interestingly, decrease of 5-HT_{1A} receptor BP_{ND} is a core biomarker of these pathologic conditions (3, 22). Therefore, OXT effect on the serotoninergic system expressed as an increase of 5-HT_{1A} receptors BP_{ND} might be crucial for predicting adaptive responses to social environments. Given the two neuromodulators' implication in emotion-based behavior and psychiatric disorders, OXT and 5-HT systems should probably be considered jointly as targets of future therapeutic interventions.

Materials and Methods

Subjects. A total of 24 healthy males participated in this study (mean age, 26.33 ± 6.33 y). Subjects affected by chronic diseases or mental disorders, under pharmacological medication, or with a history of smoking, drugs, or alcohol abuse were excluded. All these criteria were evaluated during the medical examination, before the beginning of the experiment. All subjects gave written, informed consent and were told of their rights to discontinue participation at any time. The study was approved by the ethical committee for biomedical research (Comité de Protection des Personnes SUD EST IV no. 10/040–2010-019922–1; Agence Nationale de Sécurité du Médicament, A100727-77).

Table 2. Regions correlating with the right amygdala MPPF BP_{ND} (seed region) after OXT

		Cluster peak				
				MNI coordinates (mm)		
Brain region	Cluster size, cm^3	*Z*-score	*P* value	*x*	*y*	*z*
Right Insula	4.77	3.33	< 0.001	26	8	−15
Right hippocampus	2.64	3.50	< 0.001	29	−12	−18
Left subgenual frontal cortex	4.77	5.02	<0.001	−3	16	−5
Right subgenual frontal cortex	4.77	4.40	<0.001	2	16	−5
Right medial orbital gyrus	0.70	2.63	0.004	10	52	−24
Right posterior orbital gyrus	4.77	3.32	<0.001	20	16	−12

Experimental Design. In this double- blind placebo-controlled study, subjects underwent two PET scans separated by 1 week to evaluate $5HT_{1A}$ receptors' BP_{ND} during the basal state ($n = 24$) and the effect of intranasal administration of OXT or placebo. Twelve subjects, randomly selected from the pool of the 24 participants, received a spray containing OXT, and the other 12 received a spray containing the placebo. OXT and placebo were prepared and conditioned by the pharmacist of an independent laboratory (LC2). A box containing two identical bottles, each with a printed code corresponding to OXT or placebo, was assigned to each subject. The codes were revealed by the pharmacist at the end of the study. Because specific foods can influence OXT and 5-HT synthesis, participants abstained from food and drink (other than water) for 2 h before the beginning of the experiment and from exercise, sexual relations, caffeine, tobacco, cola soft drink, tea, alcohol, chocolate, bananas, and dry fruits during the 24 h preceding the examination. If those conditions were not followed, the subject was excluded from the study.

Anatomical MRI. All subjects underwent an anatomical MRI examination performed at Centre d'Exploration et de Recherche Médicale par Emission de Positons (CERMEP) on a 1.5-T Magnetom scanner (Siemens), including a 3D anatomic T1-weighted sequence covering the whole brain volume, with 1 mm^3 cubic voxels and 176 1-mm-thick slices.

PET Sessions. ***PET scan sequence.*** PET scan session always started at 12:30 PM. During the 60-min PET acquisition, subjects were lying at rest in the machine. ***Basal PET scan.*** The day of the basal examination, subjects were conducted to the imagery center (CERMEP) at 11:50 AM. They were quietly installed in the machine, and then the i.v. catheter, necessary for the injection of the radioligand, was placed in a vein of the left forearm at approximately 12:00 PM. ***Spray PET scan.*** The day of the spray administration, subjects were brought to the CERMEP imaging center at 11:00 AM. For the basal PET scan, patients were quietly placed in the scanner, and then the i.v. catheter was placed in a vein of the left forearm at 11:10 AM. Participants were randomly assigned to the OXT or placebo group. The nasal spray was administered at 11:50 AM, 40 min before PET registration. Subjects in the OXT group received 24 IU of OXT (Syntocinon Spray; Novartis; three puffs per nostril, with each puff containing 4 IU OXT), whereas those in the placebo group received a placebo containing all the ingredients present in the OXT spray with the exception of the active OXT molecule. Afterward, the participants were comfortably installed in a quiet room until the beginning of the registration, which took place 40 min later.
[^{18}F]MPPF PET. [^{18}F]MPPF was obtained by nucleophilic fluoration of a nitro precursor with a radiochemical yield of 20–25% at the end of the synthesis and a specific activity of 32–76 GBq/mmol (50, 51).

Data Acquisition. PET scans were obtained on a Biograph mCT PET-CT tomograph (Siemens). Measures for tissues and head support attenuation were performed with a 1-min low-dose CT scan acquired before emission data acquisition. A bolus of [^{18}F]MPPF at 2.7 MBq/kg was injected through an i.v. catheter placed in a vein of the left forearm (mean injected dose, 192 MBq for control subjects and 184 MBq for patients). A dynamic emission scan was acquired in list mode during the 60 min after injection. A total of 35 frame images were reconstructed by using the 3D-ordinary Poisson-ordered subset expectation maximization iterative algorithm incorporating PSF and time of flight (with a Gaussian filter of 3 mm) after correction for scatter and attenuation [128×128 voxels in-plane (2.12 mm^2) and 109 slices (2.03-mm thickness)]. The resolutions for reconstructed images were approximately 2.6 mm in full width at half maximum in the axial direction and 3.1 mm in full width at half maximum in the transaxial direction for a source located 1 cm from the field of view (52, 53).

Data Processing and ROI Definition. For each subject, the T1 MRI image was anatomically segmented by using the multiatlas propagation with enhanced registration method (54) based on a the Hammersmith maximum probability brain atlas, defining 83 regions (25, 55). Anatomical and segmented images were then coregistered, with mutual information criteria, to the PET image by using Statistical Parametric Mapping 8 (SPM8) software (Wellcome Trust Centre of Neuroimaging; www.fil.ion.ucl.ac.uk/spm/software/spm8/). The set of regions were chosen according to the known circuit $5\text{-}HT_{1A}$ receptor described in the literature and clearly identified in a healthy population database (24) and from basal state results obtained in our subjects (Fig. 1, *Upper*). These ROIs include the amygdala, the hippocampus, the parahippocampus, the insula, the anterior/medial cingulate area, the orbitofrontal cortex, and the DRN. These ROIs were used for subsequent regional BP_{ND} and SPM analyses.

As the Hammersmith N30R83 atlas does not provide a description of the raphe nuclei, we defined the DRN region on the basis of our PET functional data obtained in the basal state. On the average MPPF BP_{ND} image from the 24 subjects, within the limits of the brainstem region delineated by the Hammersmith atlas, we selected the cluster of voxels exceeding 80% of the maximum. This cluster was considered as belonging to DRN and so labeled.

Modeling of [^{18}F]MPPF. Parametric BP_{ND} images were computed at the voxel level. Modeling of [^{18}F]MPPF kinetic was performed by using a three-compartment simplified reference tissue model (56). In this model, the assessment of free and nonspecific ligands kinetics is based on the time–activity curve of a reference region (i.e., cerebellar white matter) that is devoid of specific $5\text{-}HT_{1A}$ receptor binding (57).

BP_{ND} images were spatially normalized into a standard Montreal Neurological Institute (MNI)/International Consortium for Brain Mapping stereotactic space by using SPM8. Deformation fields from subjects' space to MNI space were determined from the T1 MRI image by using the New Segment function of SPM8, and then applied to the raw BP_{ND} images. Normalized images were smoothed by using an isotropic Gaussian kernel of 8 mm in full width at half maximum.

Statistical Analysis. Regional BP_{ND} values were submitted to a between-groups (OXT $\times$ placebo) and within-subjects (basal $\times$ spray) ANOVA. The relative effect of OXT administration or placebo on MPPF BP_{ND} compared with their basal states was assessed by the following *t*-contrast for the whole brain: (OXT spray − basal OXT) − (placebo spray − basal placebo). Post hoc statistics tested, by region and by group, if the regional variations of MPPF BP_{ND} between the basal and the spray condition were significantly different from zero (one-sample *t* test performed on the relative difference).

A voxel-based SPM analysis was also performed, by using a flexible factorial design, to assess the effect of OXT administration or placebo on MPPF BP_{ND} compared with the basal state. SPM of Student *t*-score (SPM-{t}) maps resulting from contrasts (basal OXT and basal placebo) were thresholded at $P < 0.01$ uncorrected for multiple comparisons. This analysis was restricted to voxels belonging to our ROI set (inclusive mask).

In a second step, we performed a correlation analysis to assess whether MPPF BP_{ND} variation obtained in the DRN after OXT was correlated with any MPPF BP_{ND} voxel values. Individual regional MPPF BP_{ND} value in DRN (seed region) was extracted and submitted to a covariate analysis in SPM (multiple regression model) at the basal state and, independently, after spray administration for both groups. Contrasts tested voxels with a positive or negative correlation with the DRN BP_{ND} value.

As we found a strong correlation between DRN and the right amygdala, we looked for a relationship between the BP_{ND} in the right amygdala (seed region) and voxels within our ROIs. Similarly, the regional MPPF BP_{ND} of the right amygdala was extracted for each subject and served as covariate of interest for a new SPM analysis. Contrasts tested voxels having a positive or negative correlation with the amygdala BP_{ND} value, in the basal condition, in the OXT and in the placebo condition. SPM-{t} maps were thresholded at $P < 0.01$.

ACKNOWLEDGMENTS. We thank Région Rhône-Alpes for supporting Centre d'Etude et de Recherche Multimodal et Pluridisciplinaire PET/CT scanner acquisition, A. Lefevre for help in testing subjects, Rolf Heckemann for performing MRI segmentation, M. Desmurget and J.-R. Duhamel for helpful suggestions, S. Thobois for clinical support during the project ethical approval, and C. Billotey for performing subjects' clinical examinations. This research was funded by Centre National de la Recherche Scientifique (A.S.), Fondation de France (A.S.), Labex Cortex (A.S.), Région Rhône-Alpes (A.S.), and a French Ministry of Research fellowship (to R.M.).

1. Bartz JA, Hollander E (2006) The neuroscience of affiliation: Forging links between basic and clinical research on neuropeptides and social behavior. *Horm Behav* 50(4): 518–528.
2. Lucki I (1998) The spectrum of behaviors influenced by serotonin. *Biol Psychiatry* 44(3): 151–162.
3. Drevets WC, et al. (2007) Serotonin-1A receptor imaging in recurrent depression: Replication and literature review. *Nucl Med Biol* 34(7):865–877.
4. Arletti R, Bertolini A (1987) Oxytocin acts as an antidepressant in two animal models of depression. *Life Sci* 41(14):1725–1730.
5. Modahl C, et al. (1998) Plasma oxytocin levels in autistic children. *Biol Psychiatry* 43(4): 270–277.
6. Zafeiriou DI, Ververi A, Vargiami E (2009) The serotonergic system: Its role in pathogenesis and early developmental treatment of autism. *Curr Neuropharmacol* 7(2): 150–157.

7. Sawchenko PE, Swanson LW, Steinbusch HW, Verhofstad AA (1983) The distribution and cells of origin of serotonergic inputs to the paraventricular and supraoptic nuclei of the rat. *Brain Res* 277(2):355–360.
8. Emiliano ABF, Cruz T, Pannoni V, Fudge JL (2007) The interface of oxytocin-labeled cells and serotonin transporter-containing fibers in the primate hypothalamus: A substrate for SSRIs therapeutic effects? *Neuropsychopharmacology* 32(5):977–988.
9. Yoshida M, et al. (2009) Evidence that oxytocin exerts anxiolytic effects via oxytocin receptor expressed in serotonergic neurons in mice. *J Neurosci* 29(7):2259–2271.
10. Eaton JL, et al. (2012) Organizational effects of oxytocin on serotonin innervation. *Dev Psychobiol* 54(1):92–97.
11. Jørgensen H, Riis M, Knigge U, Kjaer A, Warberg J (2003) Serotonin receptors involved in vasopressin and oxytocin secretion. *J Neuroendocrinol* 15(3):242–249.
12. Lee R, Garcia F, van de Kar LD, Hauger RD, Coccaro EF (2003) Plasma oxytocin in response to pharmaco-challenge to D-fenfluramine and placebo in healthy men. *Psychiatry Res* 118(2):129–136.
13. Cools R, Roberts AC, Robbins TW (2008) Serotoninergic regulation of emotional and behavioural control processes. *Trends Cogn Sci* 12(1):31–40.
14. Uvnäs-Moberg K (1998) Antistress pattern induced by oxytocin. *News Physiol Sci* 13: 22–25.
15. Davis M (1992) The role of the amygdala in fear and anxiety. *Annu Rev Neurosci* 15: 353–375.
16. Kirsch P, et al. (2005) Oxytocin modulates neural circuitry for social cognition and fear in humans. *J Neurosci* 25(49):11489–11493.
17. Lischke A, et al. (2012) Oxytocin increases amygdala reactivity to threatening scenes in females. *Psychoneuroendocrinology* 37(9):1431–1438.
18. Aznavour N, Zimmer L (2007) [18F]MPPF as a tool for the in vivo imaging of 5-HT1A receptors in animal and human brain. *Neuropharmacology* 52(3):695–707.
19. Barnes NM, Sharp T (1999) A review of central 5-HT receptors and their function. *Neuropharmacology* 38(8):1083–1152.
20. Hornung J-P (2003) The human raphe nuclei and the serotonergic system. *J Chem Neuroanat* 26(4):331–343.
21. Gross C, et al. (2002) Serotonin1A receptor acts during development to establish normal anxiety-like behaviour in the adult. *Nature* 416(6879):396–400.
22. Lanzenberger RR, et al. (2007) Reduced serotonin-1A receptor binding in social anxiety disorder. *Biol Psychiatry* 61(9):1081–1089.
23. Brett M, Anton JL, Valabregue R, Poline JB (2002) Region of interest analysis using an SPM toolbox. *Neuroimage* 16(2):1140–1141.
24. Costes N, et al. (2007) Test-retest reproducibility of 18F-MPPF PET in healthy humans: A reliability study. *J Nucl Med* 48(8):1279–1288.
25. Hammers A, et al. (2003) Three-dimensional maximum probability atlas of the human brain, with particular reference to the temporal lobe. *Hum Brain Mapp* 19(4): 224–247.
26. Friston KJ, et al. (1994) Statistical parametric maps in functional imaging: A general linear approach. *Hum Brain Mapp* 2:189–210.
27. Sibon I, et al. (2008) Decreased [18F]MPPF binding potential in the dorsal raphe nucleus after a single oral dose of fluoxetine: A positron-emission tomography study in healthy volunteers. *Biol Psychiatry* 63(12):1135–1140.
28. Whitaker-Azmitia PM (2005) Behavioral and cellular consequences of increasing serotonergic activity during brain development: A role in autism? *Int J Dev Neurosci* 23(1):75–83.
29. Fisher PM, et al. (2006) Capacity for 5-HT1A-mediated autoregulation predicts amygdala reactivity. *Nat Neurosci* 9(11):1362–1363.
30. Zimmer L, Rbah L, Giacomelli F, Le Bars D, Renaud B (2003) A reduced extracellular serotonin level increases the 5-HT1A PET ligand 18F-MPPF binding in the rat hippocampus. *J Nucl Med* 44(9):1495–1501.
31. Frey BN, Rosa-Neto P, Lubarsky S, Diksic M (2008) Correlation between serotonin synthesis and 5-HT1A receptor binding in the living human brain: A combined alpha-[11C]MT and [18F]MPPF positron emission tomography study. *Neuroimage* 42(2): 850–857.
32. Udo de Haes JI, et al. (2002) 5-HT(1A) receptor imaging in the human brain: Effect of tryptophan depletion and infusion on [(18)F]MPPF binding. *Synapse* 46(2):108–115.
33. Gozlan H, Thibault S, Laporte AM, Lima L, Hamon M (1995) The selective 5-HT1A antagonist radioligand [3H]WAY 100635 labels both G-protein-coupled and free 5-HT1A receptors in rat brain membranes. *Eur J Pharmacol* 288(2):173–186.
34. Parks CL, Robinson PS, Sibille E, Shenk T, Toth M (1998) Increased anxiety of mice lacking the serotonin1A receptor. *Proc Natl Acad Sci USA* 95(18):10734–10739.
35. Kawahara H, Yoshida M, Yokoo H, Nishi M, Tanaka M (1993) Psychological stress increases serotonin release in the rat amygdala and prefrontal cortex assessed by in vivo microdialysis. *Neurosci Lett* 162(1-2):81–84.
36. Ma QP, Yin GF, Ai MK, Han JS (1991) Serotonergic projections from the nucleus raphe dorsalis to the amygdala in the rat. *Neurosci Lett* 134(1):21–24.
37. Adolphs R (2001) The neurobiology of social cognition. *Curr Opin Neurobiol* 11(2): 231–239.
38. Riem MME, et al. (2011) Oxytocin modulates amygdala, insula, and inferior frontal gyrus responses to infant crying: A randomized controlled trial. *Biol Psychiatry* 70(3): 291–297.
39. Knobloch HS, et al. (2012) Evoked axonal oxytocin release in the central amygdala attenuates fear response. *Neuron* 73(3):553–566.
40. Monk CS (2008) The development of emotion-related neural circuitry in health and psychopathology. *Dev Psychopathol* 20(4):1231–1250.
41. Roberts AC (2011) The importance of serotonin for orbitofrontal function. *Biol Psychiatry* 69(12):1185–1191.
42. Hahn A, et al. (2009) S.04.08 Serotonin-1A receptor binding potential in dorsal raphe nuclei predicts orbitofrontal reactivity in healthy subjects. *Eur Neuropsychopharmacol* 19:S182–S183.
43. Freedman LJ, Insel TR, Smith Y (2000) Subcortical projections of area 25 (subgenual cortex) of the macaque monkey. *J Comp Neurol* 421(2):172–188.
44. Drevets WC, et al. (1997) Subgenual prefrontal cortex abnormalities in mood disorders. *Nature* 386(6627):824–827.
45. Mayberg HS, et al. (2005) Deep brain stimulation for treatment-resistant depression. *Neuron* 45(5):651–660.
46. Kim S, et al. (2013) Oxytocin and postpartum depression: Delivering on what's known and what's not. *Brain Res*, 10.1016/j.brainres.2013.11.009.
47. Tops M, van Peer JM, Korf J, Wijers AA, Tucker DM (2007) Anxiety, cortisol, and attachment predict plasma oxytocin. *Psychophysiology* 44(3):444–449.
48. McCarthy MM, McDonald CH, Brooks PJ, Goldman D (1996) An anxiolytic action of oxytocin is enhanced by estrogen in the mouse. *Physiol Behav* 60(5):1209–1215.
49. Andari E, et al. (2010) Promoting social behavior with oxytocin in high-functioning autism spectrum disorders. *Proc Natl Acad Sci USA* 107(9):4389–4394.
50. Didelot A, et al. (2010) Voxel-based analysis of asymmetry index maps increases the specificity of 18F-MPPF PET abnormalities for localizing the epileptogenic zone in temporal lobe epilepsies. *J Nucl Med* 51(11):1732–1739.
51. Le Bars D, et al. (1998) High-yield radiosynthesis and preliminary in vivo evaluation of p-[18F]MPPF, a fluoro analog of WAY-100635. *Nucl Med Biol* 25(4):343–350.
52. Jakoby BW, et al. (2011) Physical and clinical performance of the mCT time-of-flight PET/CT scanner. *Phys Med Biol* 56(8):2375–2389.
53. Martí-Climent JM, et al. (2013) [Contribution of time of flight and point spread function modeling to the performance characteristics of the PET/CT Biograph mCT scanner]. *Rev Esp Med Nucl Imagen Mol* 32(1):13–21.
54. Heckemann RA, et al.; Alzheimer's Disease Neuroimaging Initiative (2010) Improving intersubject image registration using tissue-class information benefits robustness and accuracy of multi-atlas based anatomical segmentation. *Neuroimage* 51(1):221–227.
55. Gousias IS, et al. (2008) Automatic segmentation of brain MRIs of 2-year-olds into 83 regions of interest. *Neuroimage* 40(2):672–684.
56. Gunn RN, et al. (1998) Tracer kinetic modeling of the 5-HT1A receptor ligand [carbonyl-11C] WAY-100635 for PET. *Neuroimage* 8(4):426–440.
57. Costes N, et al. (2002) Modeling [18 F]MPPF positron emission tomography kinetics for the determination of 5-hydroxytryptamine(1A) receptor concentration with multi-injection. *J Cereb Blood Flow Metab* 22(6):753–765.